Conference paper

Andreea Gabor, Corneliu Mircea Davidescu, Adina Negrea, Mihaela Ciopec, Cornelia Muntean, Narcis Duteanu* and Petru Negrea

Sorption properties of Amberlite XAD 7 functionalized with sodium β-glycerophosphate

DOI 10.1515/pac-2016-0806

Abstract: This paper presents the sorption properties of a new adsorbent material prepared by impregnating Amberlite XAD 7 polymer with sodium β-glycerophosphate. For impregnation, the pellicular vacuum solvent vaporization method was employed. The functionalization was evidenced by energy dispersive X-ray analysis. The usefulness of this material and its performances were studied for the adsorption of the rare earth element La(III) in batch experiments. The influence of various parameters affecting the adsorption of lanthanum like contact time, initial concentration, pH value, and temperature was studied. The kinetic of the adsorption process was best described by the pseudo-second-order model. Sips isotherm was found to be the best fit of the equilibrium data. The maximum adsorption capacity of the functionalized material was of 33.8 mg La(III)/g. The values of thermodynamic parameters (ΔG^o, ΔH^o, ΔS^o) showed that the adsorption process was endothermic and spontaneous. The results proved that Amberlite XAD 7 functionalized with sodium β-glycerophosphate is an efficient adsorbent for the removal of La(III) ions from aqueous solutions. Quantum chemistry was performed using Spartan software.

Keywords: Amberlite XAD 7; functionalization; lanthanum; POC-16; sodium β-glycerophosphate.

Introduction

Rare earth elements, including lanthanum, are found in the earth's crust and finding them where they can lead to an economic gain is a challenge. China is considered the country with the largest amount of exploited lanthanum (95 %) [1].

Lanthanum can deliver long-term toxic effects on humans due to accumulation, causing cancer by inhalation. Lanthanum can also be gradually accumulated in soil and groundwater presenting negative effects on humans and animals.

Due to the presence of lanthanum in household equipment such as color TV sets, fluorescent lamps, energy saving lamps and bottles, in industries such as manufacturing of optical glass, catalysts, polish glass, but also in the pharmaceutical industry in form of lanthanum carbonate, lanthanum has to be removed or recovered through different methods [2, 3].

Due to the increased demand of lanthanum separation, several physical-chemical methods such as extraction, ion exchange, co-precipitation and adsorption were developed [4–6]. One of the most convenient

Article note: A collection of invited papers based on presentations at the 16th International Conference on Polymers and Organic Chemistry (POC-16), Hersonissos (near Heraklion), Crete, Greece, 13–16 June 2016.

***Corresponding author: Narcis Duteanu,** Politehnica University of Timişoara, Faculty of Industrial Chemistry and Environmental Engineering, 2 Piata Victoriei, RO 300006 Timisoara, Romania, e-mail: narcis.duteanu@upt.ro

Andreea Gabor, Corneliu Mircea Davidescu, Adina Negrea, Mihaela Ciopec, Cornelia Muntean and Petru Negrea: Politehnica University of Timişoara, Faculty of Industrial Chemistry and Environmental Engineering, 2 Piata Victoriei, RO 300006 Timisoara, Romania

methods of separating lanthanum is adsorption using different types of materials such as activated carbon [7], functionalized magnesium silicate [5], zeolite, commercial resins of Amberlite type [8], etc.

A new generation of Amberlite (XAD) resins used in general for the removal of metal ions, is studied due to their high porosity and to improved adsorbent properties obtained through functionalization with active groups (containing nitrogen, phosphorus or sulfur) [9]. Solvent-impregnated resins (SIRs) are known as selective materials for recovering metal ions from aqueous solutions [9–14]. In the present work, magnesium silicate was functionalized with groups containing phosphorus in the form of sodium β-glycerophosphate. Sodium β-glycerophosphate is considered green, being environmentally friendly, and has applications especially in the medical field [15].

The goal of this study was to evaluate the adsorptive performance of XAD7 functionalized with β-glycerophosphate, for the removal of lanthanum from aqueous solutions. Several parameters affecting the adsorption of lanthanum (contact time, initial concentration, pH value, temperature) were studied in batch experiments. Quantum calculations were performed using Spartan software in order to evaluate the HOMO, LUMO energy, and also the band gap. These parameters can be used in order to explain the possible interaction between the adsorbent and adsorbed species [16].

Materials and methods

Functionalization and characterization of the solid support

Amberlite XAD 7 copolymer resin (Rohm and Hass Co., size 0.5–0.7 mm, surface area 380 m^2/g) was used as solid support. Amberlite XAD 7 was functionalized with sodium β-glycerophosphate by pellicular vacuum solvent vaporization, using a Heidolph rotary evaporator. 0.5 g sodium β-glycerophosphate was dissolved in 25 mL absolute ethanol (99.2 %, SC PAM Corporation SRL, Romania) and mixed with 5 g of solid support in a rotary evaporator, for 10 min, at atmospheric pressure. After that, the evaporation of the solvent occurred at 323 K and a pressure of 2 Pa.

After the functionalized material was obtained, the presence of the extractant on the surface of the support was evidenced by energy dispersive X-ray analysis (EDX) using a Quanta FEG 250 instrument.

The pH value corresponding to the point of zero charge (pH_{pzc}) of the functionalized material was determined using the batch equilibration technique [17, 18]. 0.1 g material was mixed with 25 mL of 0.01 M NaCl solutions with pH values in the range 2–12 (pH_i). pH_i was adjusted with 0.1 M NaOH or HNO_3 solutions. The suspensions were shaken for 1 h at 200 rot/min and 298 K, using a Julabo SW23 mechanical shaker bath. After that, the solid material was separated by filtration and the pH_f of the solutions was determined. For pH measurements, a CRISON MultiMeter MM41 was used.

Adsorption experiments

Adsorption experiments were carried out studying different parameters like: pH, contact time, temperature, and initial concentration of La(III). In order to study the influence of the contact time and temperature on the adsorption process, samples of 0.1 g functionalized material were mixed with 25 mL of 50 mg/L lanthanum solution for 15, 30, 45, and 60 min. This experiment was carried out at temperatures of 298 K, 308 K, and 318 K.

For studying the influence of the initial metal solution, amounts 0.1 g of material were shaken for 40 min and 298 K with 25 mL metal solution with following concentrations: 10, 50, 100, 150, 200, and 300 mg/L.

The influence of pH value on adsorption efficiency was studied and 298 K using samples of 0.1 g material, in 50 mg/L solutions with pH ranging from 2 to 6. The suspensions were shaken for 1 h.

Lanthanum solutions of different concentrations were obtained by appropriate dilution from a 1 g/L stock solution. The stock solution was prepared by dissolving the adequate amount of $LaCl_3 \cdot 7H_2O$ in distilled water.

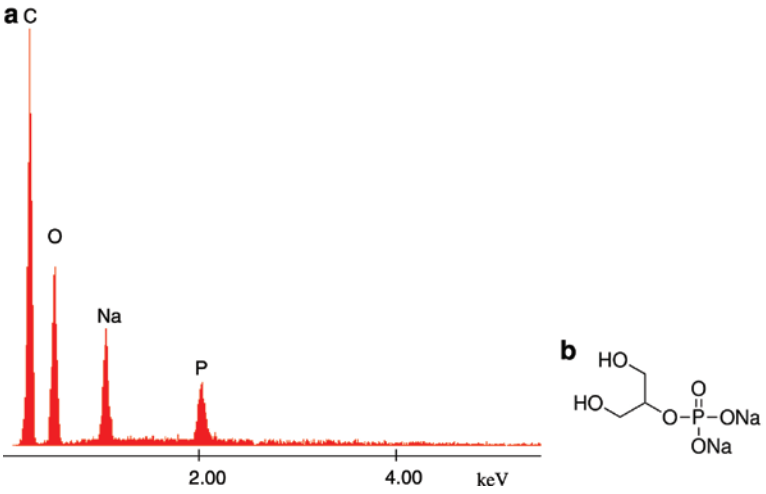

Fig. 1: (a) EDX spectrum of the functionalized material; (b) Chemical structure of sodium β-glycerophosphate.

The samples were shaken at 200 rot/min. All suspensions were filtered; the filtrate was analyzed by inductively coupled plasma mass spectrometry using an ICP-MS Bruker aurora M90 to determine the residual concentration of lanthanum.

Results and discussion

Characterization of the functionalized material

Figure 1 presents the EDX spectrum of the solid support Amberlite XAD 7 functionalized with sodium β-glycerophosphate and the chemical structure of the extractant. Specific peaks of the solid support as well as of the extractant used are visible. The presence of Na and P peaks suggest a successful functionalization of the solid support.

For the determination of pH_{pzc}, the values of the final pH (pH_f) were plotted against the values of the corresponding initial pH (pH_i) (Fig. 2). pH_{pzc} represents the ordinate of the plateau [17, 18]. For any pH_i value

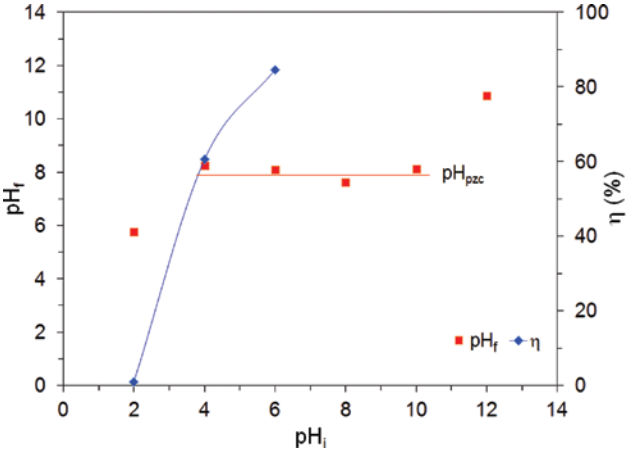

Fig. 2: pH_f versus pH_i plot for functionalized material and influence of pH on adsorption efficiency.

in this range (4–10), the material has buffering capacity and the value of pH_f is about the same, representing the pH_{pzc} (~ 8). This value of pH_{pzc} suggests that on the obtained functionalized material both anionic and cationic species can be adsorbed.

Adsorption of La(III) on the functionalized XAD 7

Influence of pH on adsorption efficiency

Figure 2 reveals that pH of the solution has a marked effect on lanthanum adsorption efficiency calculated using the following equation:

$$\eta = \frac{(C_0 - C_e)}{C_0} 100 \quad (1)$$

where C_0 is the L (III) initial concentration (mg/L) and C_e is the concentration at equilibrium (mg/L).

To avoid the precipitation of lanthanum as $La(OH)_3$, the maximum value employed for initial pH of the solution was 6. For pH values under pH_{pzc}, the surface of the material will be positively charged due to protons adsorbed, favoring the adsorption of anionic species. For pH values above pH_{pzc}, the surface will be negatively charged due to adsorption of OH^- ions from solution, and therefore the adsorption of cationic species will be favored.

The efficiency of lanthanum adsorption was maximum (~ 85 %) at $pH_i = 6$. As pH_i decreased, the positive charge of the adsorbent surface increased and therefore adsorption efficiency decreased abruptly due to electrostatic repulsion. Further experiments were carried out at pH 5–6.

Influence of initial concentration of the lanthanum solution

Figure 3 presents the influence of the initial concentration of the La(III) solution on adsorption capacity. With increase of the initial metal concentration, the adsorption capacity increased until reaching a constant value of about 34 mg/g for initial concentrations above 200 mg/L.

The equilibrium adsorption capacity was calculated using eq. 2:

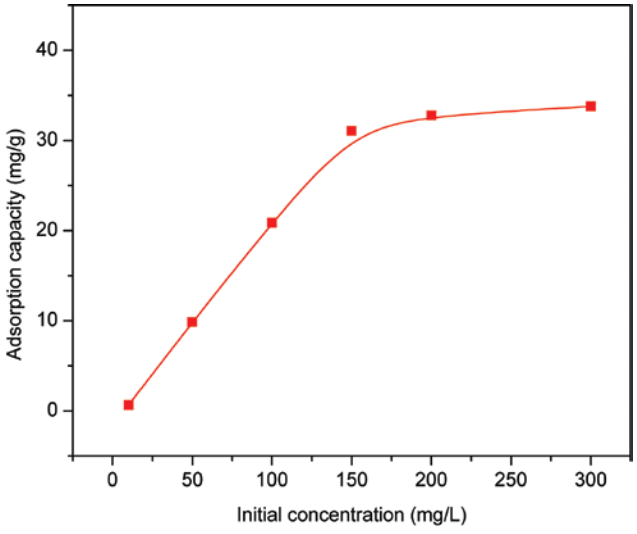

Fig. 3: Influence of the initial metal concentration on the adsorption of La(III) on the functionalized material.

$$q_e = \frac{(C_0 - C_e)V}{m} \tag{2}$$

where C_0 and C_e have the same meaning as above, V is the volume of the solution (L), and m is the amount of adsorbent material (g).

Kinetic studies and activation energy

Figure 4 presents the influence of contact time on the adsorption of La(III) onto Amberlite XAD 7 functionalized with sodium β-glycerophosphate. The adsorption capacity increased fast within the first 30 min, after which no significant changes appeared. The adsorption capacity had a slight increase with rising the temperature, suggesting that the adsorption process is endothermic in nature.

The experimental data were fitted with the Lagergren pseudo-first order kinetic model [19] and the Ho and McKay pseudo-second-order model [20] given in eqs. (3) and (4), respectively:

$$\ln(q_e - q_t) = \ln q_e - k_1 t \tag{3}$$

$$\frac{t}{q_t} = \frac{1}{k_2 q_e^2} + \frac{t}{q_e} \tag{4}$$

where q_e is the adsorption capacity at equilibrium (mg/g) and q_t is the adsorption capacity at time t, t is the contact time (min), k_1 is the pseudo-first-order rate constant (1/min) and k_2 the pseudo-second-order rate constant (g/mg·min).

For the pseudo-first order model, the linear plot $\ln(q_e - q_t)$ against t was drawn (Fig. 5). From the slope and intercept, the rate constant k_1 and the equilibrium adsorption capacity $q_{e,\,calc}$ were calculated. The linear plot t/q_t against t was drawn for the pseudo-second model (Fig. 6) and the rate constant k_2 and the equilibrium adsorption capacity $q_{e,\,calc}$ were be determined from the intercept and slope. The kinetic parameters calculated for the two kinetic models and the correlation coefficients R^2 are presented in Table 1.

Analyzing the obtained results of the two kinetic models, one can conclude that the pseudo-second order model describes better the experimental data, based on the higher correlation coefficient and the smaller difference between the experimental and calculated equilibrium adsorption capacity.

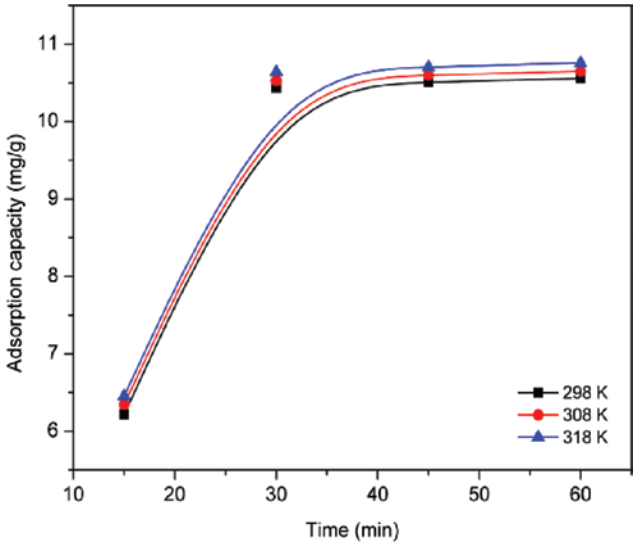

Fig. 4: Influence of contact time on the adsorption of La(III) on the functionalized material.

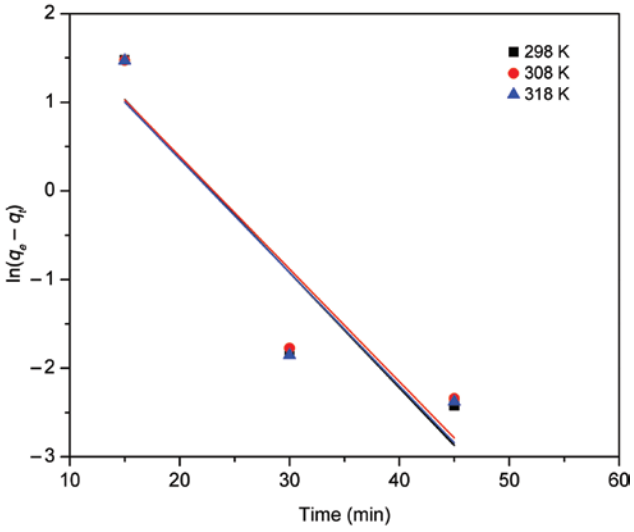

Fig. 5: Pseudo-first order plots for the adsorption of La(III) on the functionalized XAD7.

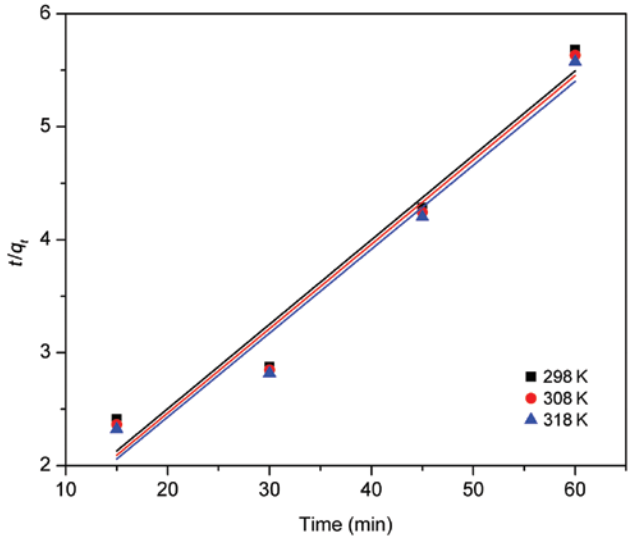

Fig. 6: Pseudo-second order plots for the adsorption of La(III) on the functionalized XAD7.

Table 1: Kinetic parameters for the adsorption of La(III) on the functionalized material.

Temperature (K)	$q_{e,exp}$ (mg/g)	k_1 (1/min)	$q_{e,calc}$ (mg/g)	R^2
Pseudo-first order				
298	10.56	0.130	19.68	0.8634
308	10.65	0.127	18.77	0.8589
318	10.76	0.128	18.65	0.8502
		k_2 (g/mg·min)		
Pseudo-second order				
298	10.56	$5.54 \cdot 10^{-3}$	13.38	0.9596
308	10.65	$5.74 \cdot 10^{-3}$	13.39	0.9621
318	10.76	$5.84 \cdot 10^{-3}$	13.46	0.9638

For the adsorption of La(III) on Amberlite XAD 7 functionalized with sodium β-glycerophosphate, the activation energy E_a (kJ/mol) was calculated using the Arrhenius equation eq. (5) and the rate constant k_2 calculated from the pseudo-second order kinetic model.

$$\ln k_2 = \ln A - \frac{E_a}{RT} \tag{5}$$

where k_2 is the rate constant (g/min·mg), A is the Arrhenius constant (g·min/mg), E is the activation energy (kJ/mol), R the ideal gas constant (8.314 J/mol·K), and T is the absolute temperature (K).

By plotting ln k_2 against $1/T$ (Fig. 7) the activation energy can be calculated. A value of 2.08 kJ/mol was obtained, which suggests a physisorption of the lanthanum ions on the functionalized material. The positive value of E_a also shows that the adsorption process is endothermic in nature [21].

Thermodynamic studies

To establish if the adsorption of La(III) on the functionalized material is spontaneous, the value of free Gibbs energy was calculated using the Gibbs–Helmholtz eq. 6:

$$\Delta G^\circ = \Delta H^\circ - T\Delta S^\circ \tag{6}$$

where ΔS° is the standard entropy change and ΔH° is the standard enthalpy change.

Using the van't Hoff equation (eq. 7) and the linear plot of lnK_d against $1/T$ (Fig. 8), the standard enthalpy change ΔH° and the standard entropy change ΔS° can be calculated.

$$\ln K_d = \frac{\Delta S^\circ}{R} - \frac{\Delta H^\circ}{RT} \tag{7}$$

where T is the absolute temperature (K) and R the ideal gas constant.

The ration between the equilibrium adsorption capacity and the equilibrium concentration represents the equilibrium constant K_d (eq. 8):

$$K_d = \frac{q_e}{C_e} \tag{8}$$

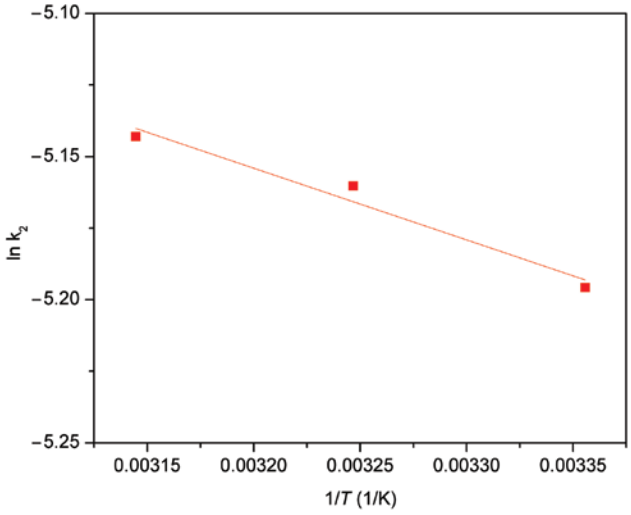

Fig. 7: Arrhenius plot of the adsorption of La(III) on the functionalized material.

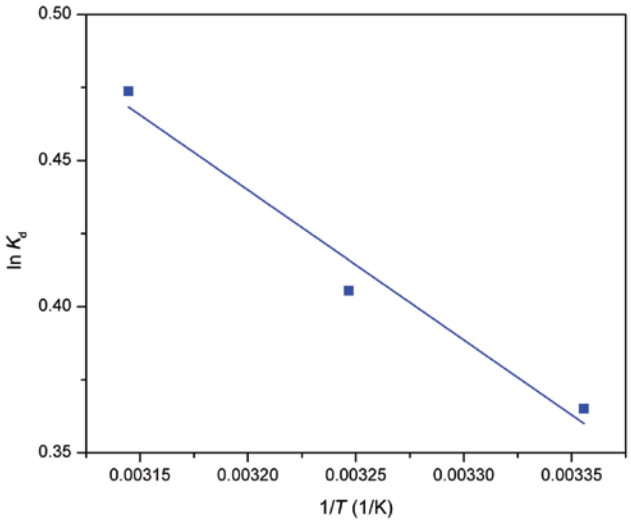

Fig. 8: Plot of ln K_d vs. $1/T$.

Table 2: Thermodynamic parameters for the adsorption of La(III) on the functionalized material.

ΔH^o (kJ/mol)	ΔS^o (J/mol·K)	ΔG^o (kJ/mol)			R^2
		298 K	308 K	318 K	
4.27	17.3	– 0.89	– 1.06	– 1.24	0.9727

The standard enthalpy change ΔH^o and the standard entropy change ΔS^o were be calculated from the intercept and slope of the linear plot of ln K_d against $1/T$ (Fig. 8). Table 2 summarizes the calculated thermodynamic parameters.

The negative values obtained for the free Gibbs energy suggest that the adsorption of La(III) on the functionalized material is spontaneous. By increasing the temperature, the free Gibbs energy becomes more negative suggesting that the adsorption is more favorable at higher temperature. The positive value of ΔH^o confirms the endothermic nature of the process, suggested by the slight increase of equilibrium adsorption capacity (q_e) and pseudo second order rate constant (k_2) with increasing temperature. The value of ΔH^o in the range 2.1–20.9 kJ/mol suggests physical adsorption. The standard entropy change ΔS^o has a positive value, suggesting that the adsorption determines a higher randomness at the solution/solid interface. However, the value of ΔS^o is very low, indicating that no remarkable changes in entropy occur [21, 22].

Equilibrium studies

The adsorption isotherm of La(III) onto XAD 7 functionalized with sodium β-glycerophosphate is presented in Fig. 9. It can be observed that as the initial concentration of La(III) increased, the adsorption capacity increased up to an equilibrium concentration of about 34 mg/g ($q_{m,\,exp}$). This value is larger than that reported previously for La(III) adsorption onto magnesium silicate functionalized with tetrabutylammonium dihydrogen phosphate (~9 mg/g) [5] and onto Amberlite XAD-4 impregnated with Aliquat-336 (~4.7 mg/g) [8].

The experimental data were fitted to three non-linear adsorption isotherm models: Langmuir, Freundlich and Sips.

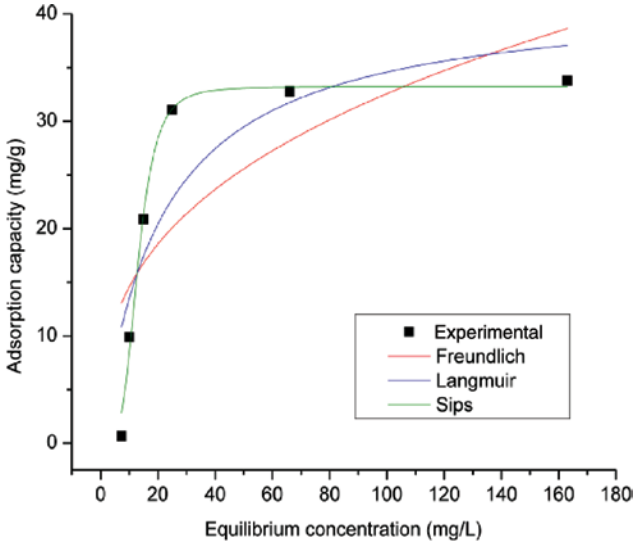

Fig. 9: Adsorption isotherm of the adsorption of La(III) on the functionalized material.

Equation 9 expresses the non-linear Langmuir isotherm [23]:

$$q_e = \frac{q_L K_L C_e}{1 + K_L C_e} \tag{9}$$

where q_e is the equilibrium adsorption capacity (mg/g), C_e is the equilibrium concentration of metal ions in the solution (mg/L), q_L the Langmuir maximum adsorption capacity (mg/g), and K_L is the Langmuir constant.

The Freundlich non-linear isotherm is written as in eq. 10 [24]:

$$q_e = K_F C_e^{1/n_F} \tag{10}$$

where q_e is the equilibrium adsorption capacity (mg/g), C_e is the equilibrium concentration of metal ions in the solution (mg/L), K_F and n_F are characteristic constants.

The Sips non-linear isotherm is written as in eq. 11 [25]:

$$q_e = \frac{q_S K_S C_e^{1/n_S}}{1 + K_S C_e^{1/n_S}} \tag{11}$$

where q_S (mg/g) is the maximum adsorption capacity, K_S is a constant related to the adsorption capacity of the adsorbent, n_S is the heterogeneity factor.

Langmuir isotherm presumes that the adsorption of the adsorbate takes place as a monolayer on the homogeneous surface of the adsorbent, the activation energy for the adsorption is uniform for all adsorbed molecules, and all adsorption sites are equal. Freundlich isotherm presumes that the surface of the adsorbent is heterogeneous, the distribution of adsorption heat is non-uniform and the adsorption can take place as multilayer. Sips isotherm is a combination of the Langmuir and Freundlich isotherms, at low concentrations of the adsorbate having the characteristics of the Freundlich isotherm, and at high concentrations the characteristics of Langmuir isotherm.

Table 3 shows the adsorption parameters for the three isotherm models used to describe the adsorption process of La(III) on Amberlite XAD 7 functionalized with sodium β-glycerophosphate. The determined isotherm parameters were used to calculate the Freundlich, Langmuir and Sips plots presented in Fig. 9.

According to the obtained parameters, the non-linear Sips adsorption model represents the best fit of the experimental data. This model has the highest value of the correlation coefficient, and calculated maximum adsorption capacity (q_s) closer to the experimental value ($q_{m,\,exp}$).

Table 3: Parameters of isotherm model for the adsorption of La(III) on the functionalized material.

Langmuir isotherm			
$q_{m,exp}$ (mg/g)	K_L (L/mg)	q_L (mg/g)	R^2
33.8	0.0477	41.8	0.7216
Freundlich isotherm			
K_F (mg/g)		$1/n_F$	R^2
6.52		0.349	0.5231
Sips isotherm			
K_S	q_S (mg/g)	$1/n_S$	R^2
$2.38 \cdot 10^{-5}$	33.2	0.241	0.9866

The values smaller than 1 calculated for the parameters $1/n_F$ and $1/n_S$ indicate favorable adsorption and convex isotherm for La(III) on the functionalized material. The values of the heterogeneity factors $1/n_F$ and $1/n_S$ are between 0.2 and 0.4. Their large deviation from 1 indicates that the surface of the obtained adsorbent material is highly heterogeneous [5, 26].

Computational calculation

Quantum calculation involved in present study were performed by using the DFT method with B3LYP functional set and 6-311 G (d, p) basis set using Spartan 14 software [27].

HOMO and LUMO energy calculation is the most important parameter used into the quantum chemistry calculation [16], because these orbital are taking place into the chemical stability [28]. Highest occupied molecular orbital (HOMO) is associated with molecule affinity to donate electrons, hence the lowest unoccupied molecular orbital (LUMO) can be associated with the molecule ability to accept electrons [28–30], and the energy gap between these two orbital is related with molecular chemical stability [31, 32]. When a molecule have a small energy gap is easier polarized, which is related with a high chemical reactivity, because they easily offer electrons to acceptor molecules [16, 32]. Another parameter which characterizes the molecular charge distribution is represented by the dipole moment. In same time, molecule dipole moment is used to describe the charge movement across the studied molecule [28].

Highest occupied molecular orbital and also the lowest unoccupied molecular orbital determined for β-glycerolphosphate are shown in Fig. 10.

According to B3LYP/6-311 G (d, p) calculation, HOMO energy, LUMO energy and also the energy band gap are:

HOMO energy = – 0.23 eV
LUMO energy = 1.21 eV
Band gap (HUMO energy – LUMO energy) = – 1.44 eV

Lower energy gap is related with the charge transfer who can take place within the organic molecule [29–33]. A molecule with a small energy gap is highly polarizable and is generally associated with a high chemical reactivity [32], explaining in this way the interaction with La (III) ions.

Conclusions

This paper presents an investigation on the sorption properties of a new developed adsorbent material. Amberlite XAD 7 polymer was functionalized with sodium β-glycerophosphate by pellicular vacuum solvent

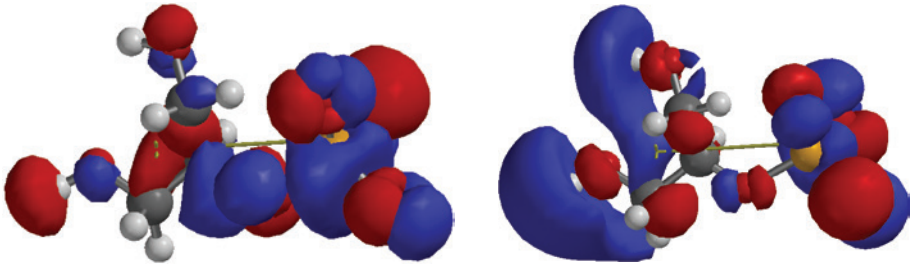

Fig. 10: HOMO – LUMO plots obtained for β-glycerolphosphate.

vaporization method. The presence of sodium β-glycerophosphate on the functionalized material was proved by EDX. The point of zero charge of the material was determined as $pH_{pzc} \sim 8$. The influence of various parameters affecting the adsorption of lanthanum like contact time, initial concentration, pH value, and temperature was studied in batch experiments. Kinetic studies showed that the optimum contact time between La(III) solution and the functionalized material was of 30 min. The data were modeled using the pseudo-first-order and the pseudo-second-order kinetic models. The kinetics of the adsorption process was best described by the pseudo-second-order model. The positive value of activation energy (2.08 kJ/mol) suggested that the adsorption process was endothermic and the mechanism was physisorption. Non-linear regression analysis of the equilibrium data was performed using Freundlich, Langmuir and Sips isotherm models. Sips isotherm was found to be the best fit of the equilibrium data. The maximum adsorption capacity of the functionalized material was of 33.8 mg La(III)/g. The values of thermodynamic parameters (ΔG^o, ΔH^o, ΔS^o) were calculated and showed that the adsorption process was endothermic and spontaneous. The results showed that Amberlite XAD 7 functionalized with sodium β-glycerophosphate is an effective adsorbent for the removal of La(III) ions from aqueous solutions. Quantum chemistry was performed using Spartan Software. Based on that were estimated the HOMO, LUMO and band gap energy.

References

[1] R. P. Wedeen, B. Berlinger, J. Aaseth, B. A. Fowler, M. Nordberg. *Handbook on the Toxicology of Metals (4th Edition)*, pp. 903–909, Academic Press, San Diego (2015).
[2] T. G. Goonan. In *U.S. Geological Survey Scientific Investigations Report 2011-5094*, p. 15, Reston (2011).
[3] C.-K. Na, H.-J. Park. *J. Hazard. Mater.* **183**, 512 (2010).
[4] Y. Li, Y. Lu, Y. Bai, W. Liao. *J. Rare Earth.* **30**, 1142 (2012).
[5] A. E. Gabor, C. M. Davidescu, A. Negrea, M. Ciopec, M. Butnariu, C. Ianasi, C. Muntean, P. Negrea. *J. Chem. Eng. Data* **61**, 535 (2016).
[6] T. J. Shaw, T. Duncan, B. Schnetger. *Anal. Chem.* **75**, 3396 (2003).
[7] E. Vences-Alvarez, L. H. Velazquez-Jimenez, L. F. Chazaro-Ruiz, P. E. Diaz-Flores, J. R. Rangel-Mendez. *J. Colloid Interf. Sci.* **455**, 194 (2015).
[8] E. A. El-Sofany. *J. Hazard. Mater.* **153**, 948 (2008).
[9] A. Ahmad, J. A. Siddique, M. A. Laskar, R. Kumar, S. H. Mohd-Setapar, A. Khatoon, R. A. Shiekh. *J. Environ. Sci.* **31**, 104 (2015).
[10] Y. Markus, A. K. SenGupta, J. A. Marinsky (Eds.). *Ion Exchange and Solvent Extraction – A Series of Advances*. CRC Press, Taylor & Francis Group (2004).
[11] R.-S. Juang. *Proc. Natl. Sci. Counc. Repub. China A* **23**, 353 (1999).
[12] M. Ciopec, C. Davidescu, A. Negrea, L. Lupa, P. Negrea, A. Popa, C. Muntean. *Environ. Eng. Manag. J.* **10**, 1597 (2011).
[13] C. M. Davidescu, M. Ciopec, A. Negrea, A. Popa, L. Lupa, P. Negrea, C. Muntean, M. Motoc. *Revista de chimie* **62**, 712 (2011).
[14] J. L. Cortina, A. Warshawsky. In *Ion Exchange and Solvent Extraction*, J. A. Marinsky, Y. Markus (Eds.), Marcel Dekker Inc., New York, NY, USA (1997).
[15] H. Y. Zhou, L. J. Jiang, P. P. Cao, J. B. Li, X. G. Chen. *Carbohyd. Polym.* **117**, 524 (2015).
[16] T. A. Yousef, O. K. Alduaij, S. F. Ahmed, G. M. Abu El-Reash, O. A. El-Gammal. *J. Mol. Struct.* **1119**, 351 (2016).

[17] A. Negrea, L. Lupa, M. Ciopec, R. Lazau, C. Muntean, P. Negrea. *Adsorpt. Sci. Technol.* **28**, 467 (2010).
[18] A. Negrea, C. Muntean, I. Botnarescu, M. Ciopec, M. Motoc. *Revista de chimie* **64**, 397 (2013).
[19] S. Lagergren. *Kungliga Svenska Vetenskapsakademiens Handlingar – Volume 24*, pp. 1–39, Royal Swedish Academy of Sciences, Stockholm, Sweden (1898).
[20] Y. S. Ho, G. McKay. *Process Biochem.* **34**, 451 (1999).
[21] P. Saha, S. Chowdhury. In *Thermodynamics*, M. Tadashi (Ed.), pp. 349–364, InTech, Rijeka, Croatia (2011).
[22] A. Negrea, M. Ciopec, C. M. Davidescu, C. Muntean, P. Negrea, L. Lupa. *Environ. Eng. Manag. J.* **12**, 991 (2013).
[23] I. Langmuir. *J. Am. Chem. Soc.* **40**, 1361 (1918).
[24] H. M. F. Freundlich. *J. Phys. Chem.* **57**, 385 (1906).
[25] R. Sips. *J. Chem. Phys.* **16**, 490 (1948).
[26] A. Negrea, L. Lupa, M. Ciopec, C. Muntean, R. Lazau, M. Motoc. *Revista de chimie* **61**, 691 (2010).
[27] W. Hehre, S. Ohlinger. *Spartan '14 for windows, Macintosh and linux – Tutorial and user guide,* Wavefunction, Inc., Irvine (2014).
[28] V. Balachandran, K. Parimala. *J. Mol. Struct.* **1007**, 136 (2012).
[29] M. Arivazhagan, R. Kavitha. *J. Mol. Struct.* **1011**, 111 (2012).
[30] S. Demir, F. Tinmaz, N. Dege, I. O. Ilhan. *J. Mol. Struct.* **1108**, 637 (2016).
[31] J. E. Galvan, D. M. Gil, H. E. Lanus, A. B. Altabef. *J. Mol. Struct.* **1081**, 536 (2015).
[32] R. Mathammal, K. Sangeetha, M. Sangeetha, R. Mekala, S. Gadheeja. *J. Mol. Struct.* **1120**, 1 (2016).
[33] T. Sivaranjani, S. Xavier, S. Periandy. *J. Mol. Struct.* **1083**, 39 (2015).